

# Instability of Baryonic Black Branes

Alex Buchel

*Department of Physics and Astronomy  
University of Western Ontario  
London, Ontario N6A 5B7, Canada  
Perimeter Institute for Theoretical Physics  
Waterloo, Ontario N2J 2W9, Canada*

## Abstract

Baryonic black branes describe the quantum critical phase of the conformal conifold gauge theory at strong coupling. This phase extends to zero temperature at a finite baryonic chemical potential, represented by extremal black branes with  $AdS_2 \times R^3 \times T^{1,1}$  throat in asymptotic  $AdS_5 \times T^{1,1}$  geometry. We demonstrate here that this phase is dynamically unstable below some critical value of  $T_c/\mu$ : the instability is represented by a diffusive mode in the hydrodynamic sound channel with a negative diffusion coefficient. We also identify a new (exotic) ordered phase of the conifold gauge theory: this phase originates at the same critical value of  $T_c/\mu$ , but extends to arbitrary high temperatures, and is characterized by an expectation value of a dimension-2 operator,  $\mathcal{O}_2 \propto T^2$ , in the limit  $\frac{\mu}{T} \rightarrow 0$ .

February 9, 2025

# Contents

<b>1</b>	<b>Introduction and summary</b>	<b>2</b>
<b>2</b>	<b>Technical details</b>	<b>5</b>
2.1	HKPT baryonic black branes . . . . .	9
2.2	Hydrodynamics of baryonic black branes . . . . .	12
2.3	Onset of spatially homogeneous instability of baryonic black branes . .	16
2.4	$R$ -symmetry charged baryonic black branes with $\mu_B \neq 0$ and $\mu_R = 0$ .	20
2.5	Non-perturbative instability of the baryonic black branes . . . . .	22
2.6	Phases of the conifold gauge theory with $\mu_B \neq 0$ and $\mu_R = 0$ . . . . .	25

## 1 Introduction and summary

In [1] (HKPT) the authors discussed an interesting top-down model of the emergent holographic criticality based on  $\mathcal{N} = 1$  superconformal  $SU(N) \times SU(N)$  Klebanov-Witten (KW) gauge theory [2]. The gauge theory has  $U(1)_R \times U(1)_B$  ( $R$ -charge and baryonic) global symmetry. There is a phase of the theory with a nonzero  $R$ -charge chemical potential  $\mu_R \neq 0$  and a vanishing baryonic chemical potential  $\mu_B = 0$ , with a holographic dual represented by Reissner-Nordstrom black branes in asymptotically  $AdS_5$  space-time. While one can reach a quantum criticality, *i.e.*, the limit of vanishing temperature with a finite entropy density, in this phase, it was expected that the corresponding extremal black branes would be unstable due to the presence of the charged under the  $R$ -symmetry matter <sup>1</sup>. Instead, the authors of [1] studied a phase of the KW gauge theory with  $\mu_R = 0$  and  $\mu_B \neq 0$  — the corresponding gravitational dual named “baryonic black branes”. It was shown that quantum criticality can be reached in this phase as well, and the authors conjectured that the absence of charged matter under  $U(1)_B$  symmetry in type IIB supergravity description<sup>2</sup> would make this phase perturbatively<sup>3</sup> stable even in the limit  $\frac{T}{\mu_B} \rightarrow 0$ .

---

<sup>1</sup>Such instabilities were indeed identified in [3].

<sup>2</sup>The gauge invariant operators with baryonic charge in KW gauge theory have conformal dimension of order  $N$ , realized by wrapped D3-branes with charge-to-mass ratio being too small to trigger the instability of the holographic superconductors [4].

<sup>3</sup>Non-perturbative “Fermi seasickness” instability [5] has been known to authors of [1] - I would like to thank Igor Klebanov for stressing this point. We comment on this instability below.

In this paper we establish that the HKPT quantum criticality is perturbatively unstable after all. The instability here parallels the recently identified instability of  $\mathcal{N} = 4$  supersymmetric Yang-Mills (SYM) theory in a phase with a diagonal  $U(1)_R$ -symmetry chemical potential [6]. Specifically, we find that the HKPT gauge theory plasma is unstable for

$$\frac{T}{\mu_B} < \frac{T}{\mu_B} \Big|_{crit} = 0.2770(5) \quad (1.1)$$

to fluctuations of a combination of a neutral dimension-2 scalar (in  $\mathcal{N} = 4$  Betti vector multiple), a  $U(1)_R$  gauge field, and a massive vector of the  $\mathcal{N} = 2$  consistent subtruncation of type IIB supergravity of warped deformed conifold with fluxes [7–9]. The instability is a diffusive mode in the hydrodynamic sound channel with a dispersion relation<sup>4</sup>

$$\mathfrak{w} = -iD\mathfrak{q}^2 + \mathcal{O}(\mathfrak{q}^2), \quad (1.2)$$

where the diffusion coefficient  $D$  vanishes at critical temperature (1.1), and

$$\begin{cases} D > 0, & \frac{T}{\mu_B} > \frac{T}{\mu_B} \Big|_{crit} \\ D < 0, & \frac{T}{\mu_B} < \frac{T}{\mu_B} \Big|_{crit} \end{cases}, \quad (1.3)$$

Much like in the case of  $\mathcal{N} = 4$  supersymmetric Yang-Mills theory [10,11], Klebanov-Witten gauge theory with a baryonic chemical potential has a spatially homogeneous exotic conformal ordered phase, originating precisely at the critical temperature (1.1). This phase extends to arbitrary high temperatures and is characterized by an expectation value of a dimension-2 operator  $\mathcal{O}_2 \propto T^2$  as  $T \gg \mu_B$ . This phase, however, never dominates in the grand canonical ensemble as it has a higher Gibbs free energy density than the corresponding HKPT baryonic black brane phase. Exotic ordered phase of the  $U(1)_B$  charged KW theory also carries  $R$ -symmetry charge density — the latter vanishes at critical temperature (1.1) as  $\propto \sqrt{T - T_{crit}}$ , exactly as the thermal expectation value of  $\mathcal{O}_2$  operator. Further details of the phases of the conifold gauge theory at  $\mu_B \neq 0$  and  $\mu_R = 0$  are collected in section 2.6.

As noted in [1], baryonic black branes suffer from the nonperturbative instability, associated with the nucleation of the a space-time filling D-brane towards the AdS

---

<sup>4</sup>We use notation  $\mathfrak{w} \equiv \frac{\omega}{2\pi T}$  and  $\mathfrak{q} \equiv \frac{|\vec{q}|}{2\pi T}$ .

boundary. We revisit this instability in section 2.5, and identify its precise onset,

$$\frac{T}{\mu_B} < \frac{T}{\mu_B} \Big|_{non-pert} = 0.2789(9) \iff \frac{T}{\mu_B} \Big|_{non-pert}^{HKPT} = \frac{0.2789(9)}{\sqrt{2}} = 0.1972(7) \approx 0.2. \quad (1.4)$$

The reported value (1.4) agrees with the one in [1]: there is a factor of  $\sqrt{2}$  difference<sup>5</sup> between the normalization of the bulk gauge field (dual to  $U(1)_B$  global symmetry) used here and in [1]. While the brane nucleation instability is first triggered at a *higher* temperature than the perturbative instability (1.1), the brane nucleation rate is suppressed both in the large- $N$  't Hooft limit, and by a spacial volume of a nucleated brane.

Section 2 collects the technical details. We begin with the review of the gravitational dual effective action of the KW gauge theory with  $U(1)_B \times U(1)_R$  global symmetries [8]. In section (2.1) we review the baryonic black branes of [1]. In section 2.2 we study the quasinormal modes of these baryonic black branes, associated with the fluctuations of the  $R$ -symmetry charge density. We show that these fluctuations become unstable below the critical temperature (1.1), leading to the clumping of the  $R$ -symmetry charges along the translationary invariant horizon of HKPT black branes. We continue the search for additional instabilities of baryonic black branes in section 2.3: analyzing the fluctuation equations (derived in section 2.2) we predict a new homogeneous phase of the conifold gauge theory plasma with a baryonic chemical potential, originating at the critical temperature (1.1). This new phase is constructed in section 2.4.

It was argued in [12] that the thermodynamic instabilities in neutral plasma always imply the dynamical instabilities of the holographic dual black branes (and of course dynamical instabilities in the boundary gauge theory plasma itself!). Extension of this argument to the charged plasma predicted the instabilities of the  $\mathcal{N} = 4$  SYM charged plasma reported in [6]. For the KW gauge theory discussed here, we explicitly demonstrated the dynamical instabilities, but we did not undertake the thermodynamic stability analysis in the presence of  $U(1)_B \times U(1)_R$  charge densities — it would be interesting to fill this gap<sup>6</sup>. Additionally, the ordered phase of the  $\mathcal{N} = 4$  SYM plasma [10] is expected to be dynamically unstable [6, 11]. We do not know if the corresponding ordered phase of the KW plasma is perturbatively stable.

---

<sup>5</sup>I would like to thank the referee for raising this possibility. See (2.28).

<sup>6</sup>While we do not expect this to be the case in the model discussed, dynamical instabilities in holographic models do not always imply the thermodynamic instabilities [13].

We would like to conclude re-emphasizing the perils of near-extremal black branes. It is natural to discuss gravitational quantum effects of the near-extremal horizons in consistent theories of quantum gravity. Embedding near-extremal horizons in String Theory necessitates introduction of additional fields. It has been known for a long time that charged matter generically destabilizes near-extremal black branes at a classical level [4]. The authors of [6] identified a new classical mechanism for the instability: the fluctuations of the 'dormant' gauge fields, required by the string theory embedding, but not activated at the background level. There is clearly a lot of similarities between the extremal horizons in  $\mathcal{N} = 4$  model and the conifold gauge theory; it would be interesting to understand the genericity of these similarities.

## 2 Technical details

The relevant effective action is the  $\mathcal{N} = 2$  consistent subtruncation of the supersymmetric consistent truncation of type IIB supergravity on warped deformed conifold with fluxes [8]:

$$S_{eff} = \frac{1}{2\kappa_5^2} \int_{\mathcal{M}_5} R \star 1 + S_{kin,scal} + S_{kin,vect} + S_{top} + S_{pot}, \quad (2.1)$$

with

$$S_{kin,scal} = -\frac{1}{2\kappa_5^2} \int_{\mathcal{M}_5} \left\{ \frac{28}{3} du^2 + \frac{4}{3} dv^2 + \frac{8}{3} dudv + 4dw^2 + \frac{1}{2} d\phi^2 + \frac{1}{2} e^{2\phi} dC_0^2 + e^{-4u-\phi} |h_1^\Omega|^2 + e^{-4u+\phi} |g_1^\Omega|^2 + 2e^{-8u} f_1^2 \right\} \star 1, \quad (2.2)$$

$$S_{kin,vect} = -\frac{1}{2\kappa_5^2} \int_{\mathcal{M}_5} \left\{ \frac{1}{2} e^{\frac{8}{3}u + \frac{8}{3}v} (dA)^2 + e^{-\frac{4}{3}u - \frac{4}{3}v} \cosh(2w) \left[ (da_1^J)^2 + (da_1^\Phi)^2 - 2 \tanh(4w) da_1^J \lrcorner da_1^\Phi \right] \right\} \star 1, \quad (2.3)$$

$$S_{top} = \frac{1}{2\kappa_5^2} \int_{\mathcal{M}_5} (A \wedge da_1^J \wedge da_1^J - A \wedge da_1^\Phi \wedge da_1^\Phi), \quad (2.4)$$

$$S_{pot} = \frac{1}{2\kappa_5^2} \int_{\mathcal{M}_5} \left\{ 24e^{-\frac{14}{3}u - \frac{2}{3}v} \cosh(2w) - 4e^{-\frac{20}{3}u + \frac{4}{3}v} \cosh(4w) - 2e^{-\frac{32}{3}u - \frac{8}{3}v} f_0^2 - e^{-\frac{20}{3}u - \frac{8}{3}v} \left[ e^{-\phi} |h_0^\Omega|^2 + e^\phi |g_0^\Omega|^2 \right] \right\} \star 1. \quad (2.5)$$

Various fields in (2.1) uplifts to 10d type IIB supergravity as follows:

- The 10d Einstein frame metric is a direct warped product of metric on  $\mathcal{M}_5$  and a metric on the deformed coset

$$T^{1,1} \equiv \frac{SU(2) \times SU(2)}{U(1)}, \quad (2.6)$$

parameterized by three 0-forms  $\{u, v, w\}$  and a single 1-form  $A$  on  $\mathcal{M}_5$ ,

$$ds_{10}^2 = e^{-\frac{8}{3}u - \frac{2}{3}v} \cdot \underbrace{ds_5^2}_{\text{metric on } \mathcal{M}_5} + \underbrace{\sum_{I=1}^5 E^I E^I}_{\text{metric on } T^{1,1}}, \quad (2.7)$$

$$\sum_{I=1}^5 E^I E^I \equiv \frac{1}{6} e^{2u+2w} (e_1^2 + e_2^2) + \frac{1}{6} e^{2u-2w} (e_3^2 + e_4^2) + \frac{1}{9} e^{2v} (e_5 - 3A)^2,$$

where  $e_i$  are the standard coframe 1-forms on  $T^{1,1}$  [14],

$$\begin{aligned} e_1 &= -\sin \theta_1 d(\phi_1), & e_2 &= d(\theta_1), \\ e_3 &= \cos \psi \sin \theta_2 d(\phi_2) - \sin \psi d(\theta_2), \\ e_4 &= \sin \psi \sin \theta_2 d(\phi_2) + \cos \psi d(\theta_2), \\ e_5 &= d(\psi) + \cos \theta_1 d(\phi_1) + \cos \theta_2 d(\phi_2), \end{aligned} \quad (2.8)$$

for angular coordinates  $\{\theta_1, \phi_1, \theta_2, \phi_2, \psi\}$  with ranges  $0 \leq \theta_{1,2} < \pi$ ,  $0 \leq \phi_{1,2} < 2\pi$ , and  $0 \leq \psi < 4\pi$ .

- $\phi$  and  $C_0$  are type IIB dilaton and axion.
- To parameterize NSNS and RR 3-form fluxes we introduce left-invariant 1- and 2-forms on the coset,

$$\eta = -\frac{1}{3} e_5, \quad \Omega = \frac{1}{6} (e_1 + i e_2) \wedge (e_3 - i e_4). \quad (2.9)$$

- NSNS 2-form potential  $B_2$  and a 3-form flux  $H_3$  are parameterized by a complex 0-form  $b^\Omega$  on  $\mathcal{M}_5$ :

$$H_3 = d(B_2), \quad B_2 = \text{Re}(b^\Omega \Omega). \quad (2.10)$$

The field strength  $H_3$  can be decomposed in a basis of left-invariant forms on  $T^{1,1}$  (2.9):

$$H_3 = \text{Re} [h_1^\Omega \wedge \Omega + h_0^\Omega \Omega \wedge (\eta + A)], \quad (2.11)$$

where we defined

$$h_1^\Omega = db^\Omega - 3i A b^\Omega \equiv Db^\Omega, \quad h_0^\Omega = 3i b^\Omega. \quad (2.12)$$

■ RR 2-form potential  $C_2$  and a 3-form flux  $F_3$  are parameterized by a complex 0-form  $c^\Omega$  on  $\mathcal{M}_5$ :

$$F_3 = d(C_2) - C_0 H_3, \quad C_2 = \text{Re}(c^\Omega \Omega). \quad (2.13)$$

The field strength  $F_3$  can be decomposed in a basis of left-invariant forms on  $T^{1,1}$  (2.9):

$$F_3 = \text{Re} [g_1^\Omega \wedge \Omega + g_0^\Omega \Omega \wedge (\eta + A)], \quad (2.14)$$

where we defined

$$g_1^\Omega = dc^\Omega - 3i A c^\Omega - C_0 Db^\Omega \equiv Dc^\Omega - C_0 Db^\Omega, \quad g_0^\Omega = 3i (c^\Omega - C_0 b^\Omega). \quad (2.15)$$

- The remaining fields of the effective action (2.1), *i.e.*, the 0-form  $f_0$  (in  $S_{pot}$ , see (2.5))

$$f_0 = k + 3\text{Im} [b^\Omega \overline{c^\Omega}], \quad (2.16)$$

and the 1-form  $f_1$  (in  $S_{kin,scal}$ , see (2.2))

$$f_1 = d(a) - 2a_1^J - kA + \frac{1}{2} \left[ \text{Re} [b^\Omega \overline{Dc^\Omega}] - b \leftrightarrow c \right], \quad (2.17)$$

are parameterized by a constant  $k$ , and additional 0-form  $a$  and a 1-form  $a_1^J$ .  $f_0$ ,  $f_1$  and the remaining 1-form  $a_1^\Phi$  describe the self-dual 5-form field strength of type IIB supergravity<sup>7</sup>.

- The 5d gravitational coupling  $\kappa_5$  is related to the Klebanov-Witten gauge theory central charge  $c_{KW}$  as follows:

$$\kappa_5^2 = \frac{\pi^2}{c_{KW}}, \quad c_{KW} = \frac{27}{64} N^2. \quad (2.18)$$

---

<sup>7</sup>For detailed discussion see section 2.4 of [9].

10d type IIB supergravity is invariant under  $SL(2, \mathbb{R})$  duality transformation. This duality is inherited by the consistent truncation (2.1). As a result, we can always work in a duality frame with

$$C_0 \equiv 0, \quad (2.19)$$

which we will do from now on. The last step is to turn off 3-form fluxes:

$$b^\Omega = c^\Omega = 0, \quad (2.20)$$

which is a consistent truncation; which in turn implies that the dilaton is constant — without loss of generality we set from now on

$$\phi = 0. \quad (2.21)$$

Effective action (2.1) is invariant under the 1-form gauge transformations (with the 0-form gauge parameters  $\alpha, \beta$  and  $\gamma$ ):

$$\begin{aligned} (I) : A &\rightarrow A + d\alpha, & a &\rightarrow a + k\alpha, \\ (II) : a_1^J &\rightarrow a_1^J + d\beta, & a &\rightarrow a + 2\beta, \\ (III) : a_1^\Phi &\rightarrow a_1^\Phi + d\gamma. \end{aligned} \quad (2.22)$$

Note that using the bulk gauge transformation we can set  $a = 0$ . We will keep the scalar  $a$  for now, and later fix the gauge transformations as convenient.

As explained in [3], setting a constant  $k = 2$  sets the asymptotic  $AdS_5$  radius  $L = 1$ . Furthermore, it is convenient to introduce the linear combinations of the vector fields as

$$A = \frac{1}{3}\mathcal{A} + \frac{2}{3}\mathcal{V}, \quad a_1^J = \frac{1}{3}\mathcal{V} - \frac{1}{3}\mathcal{A}, \quad (2.23)$$

so that  $\mathcal{A}$  is a graviphoton of the minimal  $\mathcal{N} = 2$  gauged supergravity from the consistent truncation of type IIB theory on Sasaki-Einstein manifolds with 5-form flux [15], and  $\mathcal{V}$  is a massive vector dual to a gauge theory operator  $\mathcal{O}_\mathcal{V}$  of conformal dimension 7. Finally, the graviphoton is dual to the conserved  $R$ -symmetry current of the global  $U(1)_R$ , and the massless bulk vector  $a_1^\Phi$  is dual to the conserved current of the baryonic  $U(1)_B$  symmetry.

To summarize, the effective action  $S_5$  dual to Klebanov-Witten  $\mathcal{N} = 1$  SCFT, which is relevant to study of its thermal equilibrium states with finite  $U(1)_B$  baryonic chemical potential is a functional of a 5d metric, 3 vector fields, and 4 real scalar fields<sup>8</sup>:

$$S_5 \left[ g_{\mu\nu}; \underbrace{u, v, w}_{\text{geometry}}, a; a_1^\Phi, \mathcal{A}, \mathcal{V} \right] = S_{eff} \Big|_{b^\Omega=c^\Omega=\phi=0, k=2}. \quad (2.24)$$

---

<sup>8</sup>As it was pointed out in [8], this is *A More General Consistent Truncation* of section 7.1 of [1].

The HKPT effective action  $S_{HKPT}$ , used to construct baryonic black branes in [1], is a further consistent truncation of (2.24):

$$\begin{aligned}
S_{HKPT} \left[ g_{\mu\nu}; \underbrace{u, v}_{\text{geometry}}; a_1^\Phi \right] &= S_5 \Big|_{A=\mathcal{V} \equiv 0, w=a \equiv 0} \\
&= \frac{1}{2\kappa_5^2} \int_{\mathcal{M}_5} \left\{ R - \frac{28}{3} du^2 - \frac{4}{3} dv^2 - \frac{8}{3} dudv - e^{-\frac{4}{3}u - \frac{4}{3}v} (da_1^\Phi)^2 - V(u, v) \right\} \star 1, \quad (2.25) \\
V(u, v) &= -24e^{-\frac{14}{3}u - \frac{2}{3}v} + 4e^{-\frac{20}{3}u + \frac{4}{3}v} + 8e^{-\frac{32}{3}u - \frac{8}{3}v}.
\end{aligned}$$

Eq. (2.25) reproduces the effective HKPT Lagrangian [1],

$$\begin{aligned}
\mathcal{L}_{eff} &= R - \frac{1}{4} e^{-\frac{4}{3}\chi + 2\eta} (F_{\mu\nu}^{HKPT})^2 - 5(\partial_\mu \eta)^2 - \frac{10}{3} (\partial_\mu \chi)^2 - V^{HKPT}(\eta, \chi), \quad (2.26) \\
V^{HKPT}(\eta, \chi) &= 8e^{-\frac{20}{3}\chi} + 4e^{-\frac{8}{3}\chi} (e^{-6\eta} - 6e^{-\eta}),
\end{aligned}$$

provided we identify

$$\eta = \frac{2}{5}(u - v), \quad \chi = \frac{2}{5}(v + 4u), \quad \frac{A_\mu^{HKPT}}{\sqrt{2}} = a_{1,\mu}^\Phi. \quad (2.27)$$

The factor of  $\sqrt{2}$  difference in the normalization of the HKPT bulk gauge field  $F^{HKPT}$  and  $da_1^\Phi$  implies that baryonic chemical potential  $\mu^{HKPT}$  used in [1] is related to the corresponding chemical potential  $\mu$  used here (see (2.38)) as

$$\mu^{HKPT} = \sqrt{2} \mu. \quad (2.28)$$

## 2.1 HKPT baryonic black branes

In this section we discuss the thermodynamics of the HKPT baryonic black branes. To consider  $U(1)_B$ -charged black branes in  $S_{HKPT}$  (2.25), which realize the gravitational dual to equilibrium thermal states of the KW gauge theory plasma at finite baryonic chemical potential, we take the following ansatz:

$$\begin{aligned}
ds_5^2 &= g_{\mu\nu} dx^\mu dx^\nu = -\hat{c}_1^2 dt^2 + \hat{c}_2^2 d\mathbf{x}^2 + \hat{c}_3^2 dr^2, \quad \hat{c}_i = \hat{c}_i(r), \\
a_1^\Phi &= \Phi(r) dt + a_{1,r}^\Phi(r) dr, \quad \{u, v\} = \{u, v\}(r).
\end{aligned} \quad (2.29)$$

Using the gauge transformation (III) in (2.22) we can set  $a_{1,r}^\Phi \equiv 0$ .

It is convenient to introduce

$$\begin{aligned}
v &\equiv \ln f_1, \quad u \equiv \ln f_2, \\
\hat{c}_1 &\equiv c_1 f_1^{1/3} f_2^{4/3}, \quad \hat{c}_2 \equiv c_2 f_1^{1/3} f_2^{4/3}, \quad \hat{c}_3 \equiv c_3 f_1^{1/3} f_2^{4/3}, \\
c_1 &= \frac{\sqrt{f}}{\sqrt{r}}, \quad c_2 = \frac{1}{\sqrt{r}}, \quad c_3 = \frac{s}{2r\sqrt{r}}.
\end{aligned} \quad (2.30)$$

From (2.25) we obtain the following equations of motion:

$$0 = f_1'' - \frac{9r}{16f_2^4 f f_1} (\Phi')^2 - \frac{3f_1}{4f_2^2} (f_2')^2 + \frac{7f_1' f_2'}{2f_2} + \left( \frac{f_1}{r f_2} - \frac{f_1 f_1'}{4f f_2} \right) f_2' + \left( \frac{15f'}{16f} - \frac{s'}{s} - \frac{3}{4r} \right) f_1' + \frac{1}{32f r^2 f_2^8 f_1} \left( 3f' f_2^8 f_1^2 r - 6f_2^8 f_1^2 f + 12s^2 f_2^6 f_1^2 - 34s^2 f_2^4 f_1^4 + 28s^2 \right), \quad (2.31)$$

$$0 = f_2'' + \frac{9}{4f_2} (f_2')^2 + \left( \frac{3f'}{4f} - \frac{s'}{s} + \frac{f_1'}{2f_1} \right) f_2' + \left( \frac{f_2}{4r f_1} - \frac{f_2 f_1'}{16f f_1} \right) f_1' - \frac{r}{16f_2^3 f f_1^2} (\Phi')^2 + \frac{1}{32f r^2 f_2^7 f_1^2} \left( 3f' f_2^8 f_1^2 r - 6f_2^8 f_1^2 f - 36s^2 f_2^6 f_1^2 + 14s^2 f_2^4 f_1^4 + 28s^2 \right), \quad (2.32)$$

$$0 = \Phi'' - \left( \frac{s'}{s} + \frac{f_1'}{f_1} \right) \Phi', \quad (2.33)$$

$$0 = f' + \frac{2}{r f_1 f_2^7 (-2f_2 f_1' r - 8f_1 f_2' r + 3f_2 f_1)} \left( -8f_2^7 f_1 f_2' f_1' r^2 - 12f_2^6 f_1^2 (f_2')^2 f r^2 + 4f_2^8 f_1 f f_1' r + 16f_2^7 f_1^2 f_2' f r - 3f_2^8 f_1^2 f + 6s^2 f_2^6 f_1^2 - s^2 f_2^4 f_1^4 - (\Phi')^2 f_2^4 r^3 - 2s^2 \right), \quad (2.34)$$

$$0 = s' + \frac{s}{f_2^8 f_1^2 f r (-2f_2 f_1' r - 8f_1 f_2' r + 3f_2 f_1)} \left( 2f_2^9 f_1 f (f_1')^2 r^2 + 8f_2^7 f_1^3 (f_2')^2 f r^2 + f_2^9 f_1^2 f f_1' r + 4f_2^8 f_1^3 f_2' f r + 12s^2 f_2^7 f_1^3 - 2s^2 f_2^5 f_1^5 - 2(\Phi')^2 f_2^5 f_1' r^4 - 8(\Phi')^2 f_2^4 f_1 f_2' r^4 + (\Phi')^2 f_2^5 f_1 r^3 + 4s^2 f_2 f_1' r + 16s^2 f_1 f_2' r - 10s^2 f_2 f_1 \right). \quad (2.35)$$

The equations of motion (2.31)-(2.35) describing baryonic black branes are solved subject to the following asymptotics:

- in the UV, *i.e.*, as  $r \rightarrow 0_+$ ,

$$f = 1 + f_4 r^2 + \frac{2}{3} a_2^2 r^3 + \mathcal{O}(r^5), \quad (2.36)$$

$$s = 1 + \frac{7}{30} a_2^2 r^3 - 15f_{1,8} r^4 + \mathcal{O}(r^5), \quad (2.37)$$

$$\Phi = \mu + a_2 r + \left( \frac{5}{96} a_2^3 + \frac{1}{4} a_2 f_{1,6} + \frac{1}{40} a_2^3 \ln r \right) r^4 + \mathcal{O}(r^5), \quad (2.38)$$

$$f_1 = 1 + \left( f_{1,6} + \frac{1}{10} a_2^2 \ln r \right) r^3 + f_{1,8} r^4 + \mathcal{O}(r^5 \ln r), \quad (2.39)$$

$$f_2 = 1 + \left( -\frac{1}{4}f_{1,6} - \frac{1}{40}a_2^2 - \frac{1}{40}a_2^2 \ln r \right) r^3 + f_{1,8} r^4 + \mathcal{O}(r^5 \ln r), \quad (2.40)$$

specified by

$$\left\{ a_2, f_4, f_{1,6}, f_{1,8} \right\}, \quad (2.41)$$

as functions of a  $U(1)_B$  chemical potential  $\mu$ ;

■ in the IR, *i.e.*, as  $y \equiv 1 - r \rightarrow 0_+$ ,

$$\begin{aligned} f_1 &= f_{1,0}^h + \mathcal{O}(y), & f_2 &= f_{2,0}^h + \mathcal{O}(y), & s &= s_0^h + \mathcal{O}(y), \\ \Phi &= a_1^h y + \mathcal{O}(y^2), & f &= \frac{2(s_0^h)^2 - (a_1^h)^2 (f_{2,0}^h)^4}{(f_{2,0}^h)^8 (f_{1,0}^h)^2} y + \mathcal{O}(y^2), \end{aligned} \quad (2.42)$$

specified by

$$\left\{ s_0^h, f_{1,0}^h, f_{2,0}^h, a_1^h \right\}, \quad (2.43)$$

again, as functions of a  $U(1)_B$  chemical potential  $\mu$ . Note that in total, we have 4 parameters in the UV (2.41) and 4 parameters in the IR (2.43), precisely as needed to specify a solution of a coupled system of 3 second order ODEs (2.31)-(2.33), and a pair of first order ODEs (2.34) and (2.35), given a value of the baryonic chemical potential  $\mu$ .

In practice, we solve equations of motion for  $f, s, \Phi, f_1, f_2$  using the shooting method codes adopted from [16]. Once baryonic black brane solutions are constructed, we can use the holographic renormalization<sup>9</sup> to extract their thermodynamic properties:

$$\begin{aligned} 2\pi T &= \frac{2(s_0^h)^2 - (a_1^h)^2 (f_{2,0}^h)^4}{(f_{2,0}^h)^8 (f_{1,0}^h)^2 s_0^h}, & \hat{\mathcal{E}} &\equiv 2\kappa_5^2 \mathcal{E} = -3f_4, & \hat{\rho}_B &\equiv 2\kappa_5^2 \rho_B = -4a_2, \\ \hat{\mathcal{S}} &\equiv 2\kappa_5^2 \mathcal{S} = 4\pi f_{1,0}^h (f_{2,0}^h)^4, & \hat{\Omega} &\equiv 2\kappa_5^2 \Omega = 4\mu a_2 - 3f_4 - T\hat{\mathcal{S}}, \end{aligned} \quad (2.44)$$

where  $T$  is the temperature,  $\mathcal{S}$  is the entropy density,  $\Omega$  is the Gibbs free energy density,  $\mathcal{E}$  is the energy density and  $\rho_B$  is the  $U(1)_B$  symmetry charge density. The thermodynamics of baryonic black branes is reviewed in section 2.6.

An important check on numerics is provided by enforcement of the first law of thermodynamics (A), and the conformality of the black brane phase (B):

$$\begin{aligned} (A): \quad d\hat{\Omega} &= -\hat{\mathcal{S}}dT - \hat{\rho}_B d\mu \quad \implies \quad 0 = \frac{\mu^3}{\hat{\mathcal{S}}} \cdot \left( \frac{\partial \hat{\Omega}}{\partial \mu^4} \right) \Big|_{\mu=\text{const}} + 1, \\ (B): \quad \hat{\mathcal{E}} &= 3P = -3\hat{\Omega} \quad \implies \quad 0 = \frac{\hat{\mathcal{E}}}{3\hat{\Omega}} + 1. \end{aligned} \quad (2.45)$$

---

<sup>9</sup>In this model a simple holographic renormalization of [17] is enough.

We find that the constraint (A) is satisfied at the level  $\propto 10^{-7}$ , and the constraint (B) is satisfied at the level  $\propto 10^{-11}$ .

## 2.2 Hydrodynamics of baryonic black branes

In this section we demonstrate that the HKPT baryonic black branes [1] (also reviewed in section 2.1) become dynamically unstable to spatial 'clumping' of the  $U(1)_R$  symmetry charge below the critical temperature (1.1).

Within the effective action (2.24) we consider linearized fluctuations

$$\begin{aligned} \mathcal{A} &= \delta\mathcal{A}_t dt + \delta\mathcal{A}_z dz + \delta\mathcal{A}_r dr, \quad \mathcal{V} = \delta\mathcal{V}_t dt + \delta\mathcal{V}_z dz + \delta\mathcal{V}_r dr, \quad w = \delta w, \quad a = \delta a, \\ \delta\mathcal{A}_{t,z,r} &= e^{-i\omega t + iqz} \cdot \delta\mathcal{A}_{t,z,r}(r), \quad \delta w = e^{-i\omega t + iqz} \cdot \delta W(r), \quad \delta a = e^{-i\omega t + iqz} \cdot \delta a(r), \end{aligned} \quad (2.46)$$

about the baryonic black brane background (2.29). It is straightforward to verify that the set (2.46) will decouple from the remaining fluctuations in the helicity-0 (the sound channel) sector. We use the bulk gauge transformations (2.22) to set

$$\delta\mathcal{A}_r = \delta\mathcal{V}_r \equiv 0. \quad (2.47)$$

The equations of motion for the remaining fluctuations take the form<sup>10</sup>:

$$\begin{aligned} 0 &= \delta\mathcal{A}_t'' + \left( \frac{f_1'}{3f_1} + \frac{3c_2'}{c_2} + \frac{4f_2'}{3f_2} - \frac{c_3'}{c_3} - \frac{c_1'}{c_1} \right) \delta\mathcal{A}_t' + \frac{8}{3} \left( \frac{f_1'}{f_1} + \frac{f_2'}{f_2} \right) \delta\mathcal{V}_t' + 8\Phi' \delta W' \\ &\quad - \frac{c_3^2 q}{c_2^2} (q \delta\mathcal{A}_t + \omega \delta\mathcal{A}_z) + \frac{8(f_1^4 f_2^4 - 1)c_3^2}{f_1^2 f_2^8} (i\delta a \omega + 2 \delta\mathcal{V}_t), \end{aligned} \quad (2.48)$$

$$\begin{aligned} 0 &= \delta\mathcal{A}_z'' + \left( -\frac{c_3'}{c_3} + \frac{c_2'}{c_2} + \frac{c_1'}{c_1} + \frac{f_1'}{3f_1} + \frac{4f_2'}{3f_2} \right) \delta\mathcal{A}_z' + \frac{8}{3} \left( \frac{f_1'}{f_1} + \frac{f_2'}{f_2} \right) \delta\mathcal{V}_z' \\ &\quad - \frac{8(f_1^4 f_2^4 - 1)c_3^2}{f_1^2 f_2^8} (i\delta a q - 2 \delta\mathcal{V}_z) + \frac{c_3^2 \omega}{c_1^2} (\delta\mathcal{A}_t q + \delta\mathcal{A}_z \omega), \end{aligned} \quad (2.49)$$

$$\begin{aligned} 0 &= \delta\mathcal{V}_t'' + \left( \frac{5f_1'}{3f_1} + \frac{8f_2'}{3f_2} - \frac{c_3'}{c_3} - \frac{c_1'}{c_1} + \frac{3c_2'}{c_2} \right) \delta\mathcal{V}_t' + \frac{4}{3} \left( \frac{f_1'}{f_1} + \frac{f_2'}{f_2} \right) \delta\mathcal{A}_t' - 4\Phi' \delta W' \\ &\quad - \frac{4(f_1^4 f_2^4 + 2)c_3^2}{f_1^2 f_2^8} (i\delta a \omega + 2 \delta\mathcal{V}_t) - \frac{c_3^2 q}{c_2^2} (q \delta\mathcal{V}_t + \omega \delta\mathcal{V}_z), \end{aligned} \quad (2.50)$$

---

<sup>10</sup>The background warp factors  $c_i$  are parameterized as in (2.30).

$$\begin{aligned}
0 &= \delta\mathcal{V}_z'' + \left( \frac{c'_1}{c_1} + \frac{5f'_1}{3f_1} + \frac{8f'_2}{3f_2} - \frac{c'_3}{c_3} + \frac{c'_2}{c_2} \right) \delta\mathcal{V}_z' + \frac{4}{3} \left( \frac{f'_1}{f_1} + \frac{f'_2}{f_2} \right) \delta\mathcal{A}_z' \\
&+ \frac{4(f_1^4 f_2^4 + 2)c_3^2}{f_1^2 f_2^8} (i\delta a q - 2 \delta\mathcal{V}_z) + \frac{c_3^2 \omega}{c_1^2} (q \delta\mathcal{V}_t + \omega \delta\mathcal{V}_z), \tag{2.51}
\end{aligned}$$

$$\begin{aligned}
0 &= \delta W'' + \left( \frac{4f'_2}{f_2} - \frac{c'_3}{c_3} + \frac{c'_1}{c_1} + \frac{3c'_2}{c_2} + \frac{f'_1}{f_1} \right) \delta W' + \frac{\Phi'}{3f_1^2 c_1^2 f_2^4} (\delta\mathcal{A}_t' - \delta\mathcal{V}_t') \\
&+ \left( \frac{2(\Phi')^2}{f_1^2 c_1^2 f_2^4} + \frac{c_3^2 (f_2^4 \omega^2 - 4c_1^2 (2f_1^2 - 3f_2^2))}{c_1^2 f_2^4} - \frac{c_3^2 q^2}{c_2^2} \right) \delta W, \tag{2.52}
\end{aligned}$$

$$\begin{aligned}
0 &= \delta a'' + \left( \frac{3c'_2}{c_2} - \frac{c'_3}{c_3} - \frac{4f'_2}{f_2} + \frac{c'_1}{c_1} + \frac{f'_1}{f_1} \right) \delta a' - \frac{\omega c_3^2}{c_1^2} (2i \delta\mathcal{V}_t - \delta a \omega) \\
&- \frac{c_3^2 q}{c_2^2} (\delta a q + 2i \delta\mathcal{V}_z), \tag{2.53}
\end{aligned}$$

along with the gauge fixing constraints from (2.47):

$$0 = \frac{\omega}{3} c_2^2 f_2^4 \left( 12\Phi' \delta W + \delta\mathcal{A}_t' - \delta\mathcal{V}_t' \right) + \frac{q}{3} c_1^2 f_2^4 \left( \delta\mathcal{A}_z' - \delta\mathcal{V}_z' \right) - 4i c_2^2 f_1^2 c_1^2 \delta a', \tag{2.54}$$

$$0 = \frac{\omega}{3} c_2^2 f_1^2 f_2^8 \left( \delta\mathcal{A}_t' + 2 \delta\mathcal{V}_t' \right) + \frac{q}{3} c_1^2 f_1^2 f_2^8 \left( \delta\mathcal{A}_z' + 2 \delta\mathcal{V}_z' \right) + 8i c_2^2 c_1^2 \delta a'. \tag{2.55}$$

We explicitly verified that (2.54) and (2.55) are consistent with (2.48)-(2.53).

Further introducing

$$Z_0 \equiv q \delta\mathcal{A}_t + \omega \delta\mathcal{A}_z, \quad Z_1 \equiv q \delta\mathcal{V}_t + \omega \delta\mathcal{V}_z, \quad Z_a \equiv \delta a', \quad Z_w \equiv \delta W, \tag{2.56}$$

we find from (2.48)-(2.55):

$$\begin{aligned}
0 &= Z_0'' + \left( \frac{(c_2^2 \omega^2 + c_1^2 q^2) c'_1}{c_1 (c_2^2 \omega^2 - c_1^2 q^2)} + \frac{(c_2^2 \omega^2 - 3c_1^2 q^2) c'_2}{c_2 (c_2^2 \omega^2 - c_1^2 q^2)} - \frac{c'_3}{c_3} + \frac{f'_1}{3f_1} + \frac{4f'_2}{3f_2} \right) Z_0' \\
&+ \frac{8}{3} \left( \frac{f'_1}{f_1} + \frac{f'_2}{f_2} \right) Z_1' + 8q\Phi' Z_w' + \frac{c_3^2 (c_2^2 \omega^2 - c_1^2 q^2)}{c_2^2 c_1^2} Z_0 + \frac{16c_3^2 (f_1^4 f_2^4 - 1)}{f_2^8 f_1^2} Z_1 \\
&+ \frac{16(c_2 c'_1 - c_1 c'_2) c_2 \omega q}{c_1 f_1^2 f_2^8 (c_2^2 \omega^2 - c_1^2 q^2)} \left( -i c_1^2 (f_1^4 f_2^4 - 1) Z_a + f_1^2 \Phi' f_2^8 \omega Z_w \right), \tag{2.57}
\end{aligned}$$

$$\begin{aligned}
0 &= Z_1'' + \left( \frac{(c_2^2 \omega^2 + c_1^2 q^2) c'_1}{c_1 (c_2^2 \omega^2 - c_1^2 q^2)} + \frac{(c_2^2 \omega^2 - 3c_1^2 q^2) c'_2}{c_2 (c_2^2 \omega^2 - c_1^2 q^2)} - \frac{c'_3}{c_3} + \frac{5f'_1}{3f_1} + \frac{8f'_2}{3f_2} \right) Z_1' \\
&+ \frac{4}{3} \left( \frac{f'_1}{f_1} + \frac{f'_2}{f_2} \right) Z_0' - 4q\Phi' Z_w' + c_3^2 \left( \frac{c_2^2 \omega^2 - c_1^2 q^2}{c_2^2 c_1^2} - \frac{8(f_1^4 f_2^4 + 2)}{f_1^2 f_2^8} \right) Z_1 \\
&- \frac{8(c_2 c'_1 - c_1 c'_2) c_2 \omega q}{c_1 f_1^2 f_2^8 (c_2^2 \omega^2 - c_1^2 q^2)} \left( -i c_1^2 (f_1^4 f_2^4 + 2) Z_a + f_1^2 \Phi' f_2^8 \omega Z_w \right), \tag{2.58}
\end{aligned}$$

$$\begin{aligned}
0 = & Z_w'' + \left( \frac{4f_2'}{f_2} - \frac{c_3'}{c_3} + \frac{c_1'}{c_1} + \frac{3c_2'}{c_2} + \frac{f_1'}{f_1} \right) Z_w' + \left( \frac{2(\Phi')^2}{f_1^2 c_1^2 f_2^4} + \frac{c_3^2 (f_2^4 \omega^2 - 4c_1^2 (2f_1^2 - 3f_2^2))}{c_1^2 f_2^4} \right. \\
& - \left. \frac{c_3^2 q^2}{c_2^2} \right) Z_w - \frac{\Phi'}{3f_1^2 f_2^8 c_1^2 (c_2^2 \omega^2 - c_1^2 q^2)} \left( 12c_2^2 \Phi' f_2^4 \omega^2 Z_w - 12ic_2^2 f_1^2 c_1^2 \omega Z_a \right. \\
& \left. + c_1^2 f_2^4 q (Z_0' - Z_1') \right), \tag{2.59}
\end{aligned}$$

$$\begin{aligned}
0 = & Z_a'' + \left( \frac{(3c_2^2 \omega^2 - c_1^2 q^2)c_1'}{c_1(c_2^2 \omega^2 - c_1^2 q^2)} + \frac{(3c_2^2 \omega^2 - 5c_1^2 q^2)c_2'}{c_2(c_2^2 \omega^2 - c_1^2 q^2)} - \frac{3c_3'}{c_3} + \frac{f_1'}{f_1} - \frac{4f_2'}{f_2} \right) Z_a' + \left( \frac{3(c_3')^2}{c_3^2} \right. \\
& - \frac{c_3'}{c_3} - \frac{7(\Phi')^2}{16f_1^2 c_1^2 f_2^4} + \frac{c_3^2 (c_2^2 \omega^2 - c_1^2 q^2)}{c_2^2 c_1^2} + \frac{2q^2 c_1 (c_2 c_1' - c_1 c_2')}{c_2 (c_2^2 \omega^2 - c_1^2 q^2)} \left( \frac{3c_2'}{c_2} - \frac{c_3'}{c_3} - \frac{4f_2'}{f_2} + \frac{c_1'}{c_1} + \frac{f_1'}{f_1} \right) \\
& - \frac{3c_1' c_3'}{c_1 c_3} - \frac{f_1' c_3'}{c_3 f_1} - \frac{3c_2' c_3'}{c_3 c_2} + \frac{4f_2' c_3'}{c_3 f_2} + \frac{(c_1')^2}{c_1^2} + \frac{c_1' f_1'}{8c_1 f_1} + \frac{3c_1' c_2'}{8c_1 c_2} - \frac{15c_1' f_2'}{2c_1 f_2} - \frac{(f_1')^2}{f_1^2} - \frac{45c_2' f_1'}{8f_1 c_2} \\
& + \frac{f_2' f_1'}{2f_2 f_1} - \frac{69(c_2')^2}{8c_2^2} + \frac{3c_2' f_2'}{2f_2 c_2} + \frac{67(f_2')^2}{4f_2^2} + \frac{17c_3^2 f_1^2}{4f_2^4} - \frac{51c_3^2}{2f_2^2} + \frac{25c_3^2}{2f_2^8 f_1^2} \Big) Z_a - \frac{8i\Phi' \omega c_3^2}{c_1^2} Z_w \\
& - \frac{4ic_3^2 \omega q (c_2 c_1' - c_1 c_2')}{c_2 c_1 (c_2^2 \omega^2 - c_1^2 q^2)} Z_1. \tag{2.60}
\end{aligned}$$

Solutions of (2.57)-(2.60) with appropriate boundary conditions determine the spectrum of baryonic black branes quasinormal modes — equivalently the physical spectrum of linearized fluctuations in conifold gauge theory plasma with a baryonic chemical potential (1.2). Following [18, 19] we impose the incoming-wave boundary conditions at the black brane horizon, and 'normalizability' at asymptotic  $AdS_5$  boundary. Focusing on the  $\text{Re}[\mathfrak{w}] = 0$  diffusive branch, and introducing<sup>11</sup>

$$Z_{0,1,w} = \left( \frac{c_1}{c_2} \right)^{-i\mathfrak{w}} z_{0,1,w}, \quad Z_a = \left( \frac{c_1}{c_2} \right)^{-i\mathfrak{w}-2} z_a, \quad \mathfrak{w} = -iv \mathfrak{q}, \tag{2.61}$$

we solve (2.57)-(2.60) subject to the asymptotics:

- in the UV, *i.e.*, as  $r \rightarrow 0_+$ ,

$$\begin{aligned}
z_0 &= \mathfrak{q} r + \left( \frac{1}{2} \pi^2 T^2 \mathfrak{q}^3 (v^2 + 1) - 4a_2 z_{w;2} \right) r^2 + \mathcal{O}(r^3), \\
z_1 &= -a_2 z_{w;2} r^2 + \left( z_{1;6} + \frac{7}{5} a_2 \mathfrak{q}^2 \pi^2 T^2 z_{w;2} (v^2 + 1) \ln r \right) r^3 + \mathcal{O}(r^4 \ln r), \\
z_w &= z_{w;2} r + \mathfrak{q}^2 \pi^2 T^2 z_{w;2} (v^2 + 1) r^2 + \mathcal{O}(r^3), \\
z_a &= -a_2 v T \pi z_{w;2} r^2 + \left( z_{a;6} + \frac{3}{5} a_2 v T^3 \pi^3 \mathfrak{q}^2 z_{w;2} (v^2 + 1) \ln r \right) r^3 + \mathcal{O}(r^4 \ln r), \tag{2.62}
\end{aligned}$$

---

<sup>11</sup>The shift of the IR index for  $Z_a$  is due to the fact that  $Z_a = \delta a'$ , see (2.56).

specified, for a fixed background and a momentum  $\mathbf{q}$ , by

$$\left\{ v, z_{w;2}, z_{1;6}, z_{a;6} \right\}; \quad (2.63)$$

■ in the IR, *i.e.*, as  $y \equiv 1 - r \rightarrow 0_+$ ,

$$z_{0,1,w,a} = z_{0,1,w,a;0}^h + \mathcal{O}(y), \quad (2.64)$$

specified by

$$\left\{ z_{0;0}^h, z_{1;0}^h, z_{w;0}^h, z_{a;0}^h \right\}. \quad (2.65)$$

Note that in total we have  $4+4 = 8$  parameters, see (2.63) and (2.65), which is precisely what is necessary to identify a solution of a coupled system of 4 second-order ODEs (2.57)-(2.60). Furthermore, without the loss of generality we normalized the solutions so that

$$\lim_{r \rightarrow 0} \frac{dz_0}{dr} = \mathbf{q}. \quad (2.66)$$

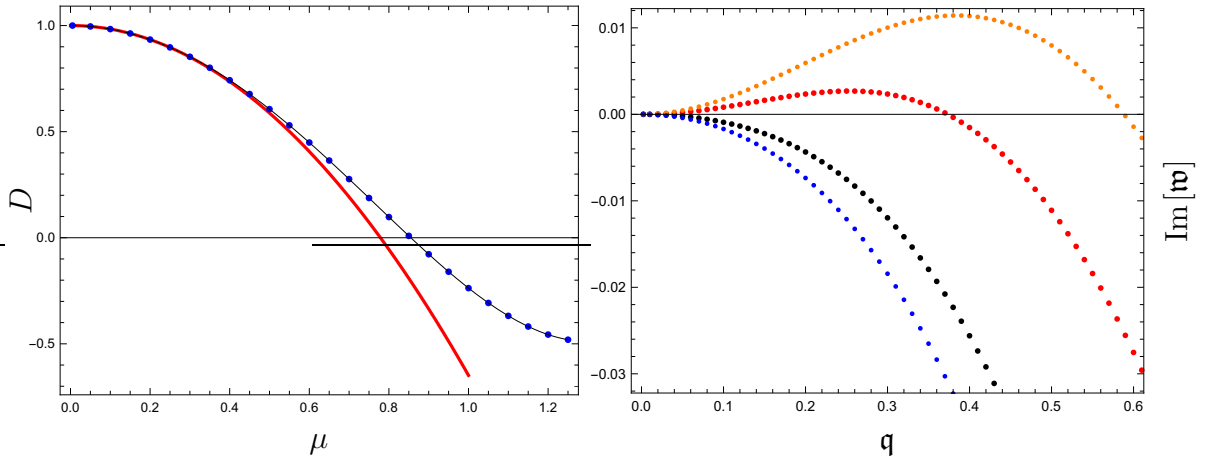


Figure 1: Left panel: the diffusive coefficient  $D$  (blue dots, see (2.67)) as a function of the baryonic chemical potential  $\mu_B$  of HKPT black branes. Its negative values indicate R-charge clumping instability of translational invariant horizons of baryonic black branes. Right panel: the imaginary part of the diffusive QNM frequency  $\mathfrak{w} = \frac{\omega}{2\pi T}$  as a function of a spatial momenta  $\mathfrak{q} = \frac{q}{2\pi T}$  for select values of  $\frac{T}{\mu_B}$  (2.70). For small values of  $\mathfrak{q}$ , the modes in plasma with  $T < T_{crit}$  (1.1) (the red and orange sets of dots) are unstable.

In practice, given a fixed baryonic black brane geometry, numerically obtained solving (2.31)-(2.35) with (2.36)-(2.40) and (2.42), we solve (2.57)-(2.60), subject to the asymptotics (2.62) and (2.64) for a range of momenta  $\mathbf{q} \in [-0.1, 0.1]$ . Obtained values of  $v \equiv v(\mathbf{q})$  allows to compute the dispersion relation for the quasinormal modes, and the diffusion coefficient in (1.2):

$$\text{Im}[\mathfrak{w}] = -v(\mathbf{q}) \cdot \mathbf{q}, \quad D = \left. \frac{dv(\mathbf{q})}{d\mathbf{q}} \right|_{\mathbf{q}=0}, \quad (2.67)$$

as functions of a baryonic chemical potential  $\mu$ . The results are these analyses are shown in fig.1. The left panel shows the diffusive coefficient  $D$  (2.67) as a function of  $\mu$  (the blue dots) — it is positive for small values of  $\mu$  (the large values of  $\frac{T}{\mu_B}$ ), and negative for sufficiently large values of the chemical potential.  $D$  vanishes at

$$\mu = \mu_* = 0.85501(6) \quad \Longrightarrow \quad \left. \frac{T}{\mu_*} = \frac{T}{\mu_B} \right|_{crit} = 0.2770(5), \quad (2.68)$$

corresponding to a critical temperature (1.1). The solid red line represents the fit to the diffusion coefficient at small  $\mu$ :

$$\left. D \right|_{red} = 1 - e^{1/2} \mu^2. \quad (2.69)$$

In the right panel we provide a sample of the dispersion relations for the modes above the critical temperature (the sets of blue and black dots), and below the critical temperature (the sets of orange and red dots):

$$\frac{T}{\mu} = \left\{ 0.8, 0.9, 1.1, 1.2 \right\} \cdot \left. \frac{T}{\mu_B} \right|_{crit}. \quad (2.70)$$

Analogously to the  $\mathcal{N} = 4$  SYM plasma discussed in [6], we find that the extremal baryonic black brane limit is never realized — there is a classical instability (at sufficiently low temperatures) in the conifold gauge theory plasma, associated with the spatial clumping of the  $U(1)_R$  symmetry charge, even though the corresponding equilibrium thermal state has only a baryonic chemical potential/charge.

### 2.3 Onset of spatially homogeneous instability of baryonic black branes

In section 2.2 we established that translationary invariant horizons of baryonic black branes become unstable below  $T_{crit}$  (1.1). Identical physical phenomenon was demonstrated in  $\mathcal{N} = 4$  SYM plasma in [6]. In the latter case, precisely at  $T_{crit}$ , there is also

an onset of a new homogeneous phase of SYM plasma<sup>12</sup> [10, 11]. In this section we establish the existence of a similar new homogeneous phase of HKPT black branes.

Since we are interested in potential instabilities leading to a homogeneous phase, we set  $q = 0$  in the equations of motion for the linearized fluctuations about the baryonic black brane background (2.48)-(2.54). This allows for a truncation with

$$\delta\mathcal{A}_z = \delta\mathcal{V}_z \equiv 0. \quad (2.71)$$

To proceed, we need to be careful with  $\omega \rightarrow 0$  limit.

- **(O-I):** We can directly set  $\omega = 0$ , which requires vanishing of  $\delta a$ , in (2.48)-(2.54) and search for the normalizable solutions of the resulting equations (as was done in [10] for a SYM),

$$\begin{aligned} 0 = \delta\mathcal{A}_t'' + \left( \frac{f_1'}{3f_1} + \frac{3c_2'}{c_2} + \frac{4f_2'}{3f_2} - \frac{c_3'}{c_3} - \frac{c_1'}{c_1} \right) \delta\mathcal{A}_t' + \frac{8}{3} \left( \frac{f_1'}{f_1} + \frac{f_2'}{f_2} \right) \delta\mathcal{V}_t' + 8\Phi' \delta W' \\ + \frac{16(f_1^4 f_2^4 - 1)c_3^2}{f_1^2 f_2^8} \delta\mathcal{V}_t, \end{aligned} \quad (2.72)$$

$$\begin{aligned} 0 = \delta\mathcal{V}_t'' + \left( \frac{5f_1'}{3f_1} + \frac{8f_2'}{3f_2} - \frac{c_3'}{c_3} - \frac{c_1'}{c_1} + \frac{3c_2'}{c_2} \right) \delta\mathcal{V}_t' + \frac{4}{3} \left( \frac{f_1'}{f_1} + \frac{f_2'}{f_2} \right) \delta\mathcal{A}_t' - 4\Phi' \delta W' \\ - \frac{8(f_1^4 f_2^4 + 2)c_3^2}{f_1^2 f_2^8} \delta\mathcal{V}_t, \end{aligned} \quad (2.73)$$

$$\begin{aligned} 0 = \delta W'' + \left( \frac{4f_2'}{f_2} - \frac{c_3'}{c_3} + \frac{c_1'}{c_1} + \frac{3c_2'}{c_2} + \frac{f_1'}{f_1} \right) \delta W' + \frac{\Phi'}{3f_1^2 c_1^2 f_2^4} (\delta\mathcal{A}_t' - \delta\mathcal{V}_t') \\ + \left( \frac{2(\Phi')^2}{f_1^2 c_1^2 f_2^4} - \frac{4c_3^2(2f_1^2 - 3f_2^2)}{c_1^2 f_2^4} \right) \delta W. \end{aligned} \quad (2.74)$$

- **(O-II):** In the limit  $\omega \rightarrow 0$ , but without directly setting  $\omega = 0$ , we can eliminate  $\delta a'$  from (2.54) and substitute the result into (2.55). We find in this case an additional first-order constraint on  $\{\delta\mathcal{A}_t, \delta\mathcal{V}_t, \delta W\}$  fluctuations, namely,

$$0 = \omega \cdot \left\{ (f_1^4 f_2^4 + 2) \delta\mathcal{A}_t' + 2(f_1^4 f_2^4 - 1) \delta\mathcal{V}_t' + 24\Phi' \delta W \right\}. \quad (2.75)$$

We kept an overall factor  $\omega$  to emphasize that (2.75) is irrelevant in the strict limit  $\omega = 0$ . It is straightforward to verify that (2.75) is consistent with the

---

<sup>12</sup>See also [20, 21] for earlier discussions.

second-order equations (2.72)-(2.73), provided we use the background equation of motion (2.33).

We show now that (2.72)-(2.73) allows for a normalizable solution, and thus for an onset of a homogeneous phase, but that this solution is inconsistent with the constraint (2.75). Physically, this suggests that the homogeneous phase predicted here (it will be further analyzed in section 2.4) can not arise from the hydrodynamic instability<sup>13</sup>.

The easiest way to identify the onset of an instability for a gravitational mode is to turn on its source term; the instability is then signalled by the divergence of its normalizable component<sup>14</sup>. Thus, we seek solutions of (2.72)-(2.74) with the following asymptotics:

- In the UV, *i.e.*, as  $r \rightarrow 0_+$ ,

$$\begin{aligned}\delta W &= (z_{w;2} + \mathbf{1} \ln r) r + \mathcal{O}(r^3 \ln r), \\ \delta \mathcal{V}_t &= \left( -a_2 z_{w;2} - \frac{7}{4} a_2 - a_2 \ln r \right) r^2 + z_{1;6} r^3 + \mathcal{O}(r^4 \ln r), \\ \delta \mathcal{A}_t &= z_{0;2} r + (-4a_2 z_{w;2} + 2a_2 - 4a_2 \ln r) r^2 + \mathcal{O}(r^4 \ln r),\end{aligned}\tag{2.76}$$

specified by

$$\left\{ z_{w;2}, z_{0;2}, z_{1;6} \right\}.\tag{2.77}$$

We highlighted the source term  $\mathbf{1}$  (which can be set to 1 as the equations are linear), and the corresponding normalizable coefficient  $z_{w;2}$ .

- In the IR, *i.e.*, as  $y \equiv 1 - r \rightarrow 0_+$ ,

$$\delta W = z_{w;0}^h + \mathcal{O}(y), \quad \delta \mathcal{A}_t = z_{0;1}^h y + \mathcal{O}(y^2), \quad \delta \mathcal{V}_t = z_{1;1}^h y + \mathcal{O}(y^2),\tag{2.78}$$

specified by

$$\left\{ z_{w;0}^h, z_{0;1}^h, z_{1;1}^h \right\}.\tag{2.79}$$

Note that in total we have  $3 + 3 = 6$  parameters ((2.77) and (2.79)), as necessary to specify a solution of a coupled system of 3 second-order ODEs (2.72)-(2.74).

If the constraint (2.75) is imposed, it determines  $\delta \mathcal{A}'_t$  algebraically from  $\delta \mathcal{V}'_t$  and  $\delta W$ , and sets

$$z_{0;2} = 0, \quad z_{0;1}^h = -\frac{2((f_{1,0}^h)^4 (f_{2,0}^h)^4 z_{1;1}^h - z_{1;1}^h + 12a_1^h z_{w;0}^h)}{(f_{1,0}^h)^4 (f_{2,0}^h)^4 + 2}.\tag{2.80}$$

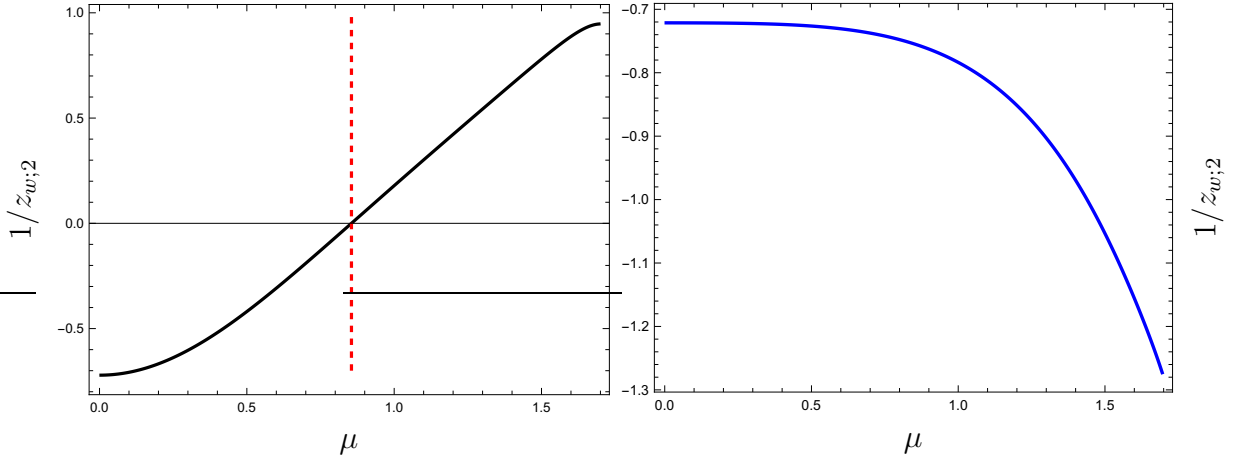


Figure 2: Left panel: the divergence of the normalizable coefficient  $z_{w;2}$  (as we vary the chemical potential  $\mu$  of the baryonic black branes) at  $\hat{\mu}_*$  (2.81) (the vertical red dashed line) signals the onset of a new homogeneous phase of the charged conifold gauge theory plasma. Right panel: such divergence is absent if the additional constraint (2.80) is used.

In fig.2 we present numerical results for the susceptibility  $\frac{1}{z_{w;2}}$  as a function of the baryonic chemical potential  $\mu$  of the conifold plasma. In the setting **(O-I)** (the left panel) there is a divergence at

$$\hat{\mu}_* = 0.855016(8), \quad (2.81)$$

indicating the onset of instability towards a homogeneous plasma phase with a finite  $R$ -symmetry charge density (since the value of  $z_{0;2} \neq 0$ ). Within numerical error, this is precisely the onset of the clumping instability identified in section 2.2. Indeed, from (2.68),

$$\frac{\hat{\mu}_*}{\mu_*} - 1 = 5.(3) \times 10^{-7}. \quad (2.82)$$

Such an instability can not arise from the hydrodynamic instability, as the susceptibility computed in the setting **(O-II)** (the right panel) remains finite.

<sup>13</sup>We believe the same is true for the ordered phase of the SYM plasma [10, 11].

<sup>14</sup>See for example section 5 of [22].

## 2.4 $R$ -symmetry charged baryonic black branes with $\mu_B \neq 0$ and $\mu_R = 0$

In this section we discuss the construction and the thermodynamics of black branes of the effective action (2.24) with a finite baryonic chemical potential  $\mu_B \neq 0$ , and a vanishing chemical potential for the  $R$ -symmetry charge,  $\mu_R = 0$ . These black branes would, nonetheless, carry the  $U(1)_R$  symmetry charge — they represent the new homogeneous and isotropic phase of the conifold gauge theory plasma that connects to the HKPT phase at the onset of the instability discussed in section 2.3.

The corresponding gravitational dual is constructed within the following ansatz:

$$\begin{aligned} ds_5^2 &= g_{\mu\nu} dx^\mu dx^\nu = -\hat{c}_1^2 dt^2 + \hat{c}_2^2 d\mathbf{x}^2 + \hat{c}_3^2 dr^2, & \hat{c}_i &= \hat{c}_i(r), \\ a_1^\Phi &= \Phi(r) dt, & \mathcal{A} &= A(r) dt, \\ \mathcal{V} &= V(r) dt + \mathcal{V}_r(r) dr, & \{u, v, w\} &= \{u, v, w\}(r), \end{aligned} \quad (2.83)$$

where we used the gauge transformations (2.22) to set  $a_{1,r}^\Phi = \mathcal{A}_r = a \equiv 0$ . From the equation of motion

$$\frac{\delta S_5}{\delta \mathcal{V}_r} = 0 \quad \Longrightarrow \quad \mathcal{V}_r \equiv 0. \quad (2.84)$$

It is convenient to introduce

$$\begin{aligned} v &\equiv \ln f_1, & u &\equiv \ln f_2, & w &\equiv \ln H, \\ \hat{c}_1 &\equiv c_1 f_1^{1/3} f_2^{4/3}, & \hat{c}_2 &\equiv c_2 f_1^{1/3} f_2^{4/3}, & \hat{c}_3 &\equiv c_3 f_1^{1/3} f_2^{4/3}, \\ c_1 &= \frac{\sqrt{f}}{\sqrt{r}}, & c_2 &= \frac{1}{\sqrt{r}}, & c_3 &= \frac{s}{2r\sqrt{r}}. \end{aligned} \quad (2.85)$$

The equations of motion for the fields in (2.85) are too long to be presented here: in summary, we have a coupled system of 6 second-order equations for  $\{f_1, f_2, \Phi, A, V, H\}$ , and a pair of the first-order equations for  $\{f, s\}$ . These equations are solved subject to the following asymptotics:

- in the UV, *i.e.*, as  $r \rightarrow 0_+$ ,

$$f = 1 + f_4 r^2 + \left( a_{t,1}^2 + \frac{2}{3} a_2^2 \right) r^3 - 2a_{t,1} h_2 a_2 r^4 + \mathcal{O}(r^5), \quad (2.86)$$

$$s = 1 - \frac{1}{2} h_2^2 r^2 + \frac{7}{30} a_2^2 r^3 + (-95h_2^4 + 19f_4 h_2^2 - 5a_2 a_{t,1} h_2 - 15f_{1,8}) r^4 + \mathcal{O}(r^5 \ln r), \quad (2.87)$$

$$\begin{aligned} \Phi = & \mu + a_2 r - 2a_{t,1}h_2 r^2 - a_2h_2^2 r^3 + \left( -\frac{1}{2}h_2^3a_{t,1} + \frac{1}{4}a_{t,1}h_2f_4 + \frac{1}{4}a_2(a_{t,1})^2 + \frac{3}{2}h_2a_{t,3} \right. \\ & \left. + \frac{5}{96}a_2^3 + \frac{1}{4}a_2f_{1,6} + \frac{1}{40}a_2^3 \ln r \right) r^4 + \mathcal{O}(r^5 \ln r), \end{aligned} \quad (2.88)$$

$$f_1 = 1 - \frac{5}{2}h_2^2 r^2 + \left( f_{1,6} + \frac{1}{10}a_2^2 \ln r \right) r^3 + f_{1,8} r^4 + \mathcal{O}(r^5 \ln r), \quad (2.89)$$

$$\begin{aligned} f_2 = & 1 + \frac{1}{2}h_2^2 r^2 + \left( -\frac{1}{4}f_{1,6} - \frac{1}{40}a_2^2 - \frac{1}{40}a_2^2 \ln r \right) r^3 + \left( \frac{1}{2}a_{t,1}a_2h_2 - \frac{3}{2}h_2^2f_4 + 9h_2^4 \right. \\ & \left. + f_{1,8} \right) r^4 + \mathcal{O}(r^5 \ln r), \end{aligned} \quad (2.90)$$

$$A = 3a_{t,1} r - 4h_2a_2 r^2 + 5h_2^2a_{t,1} r^3 + \left( 4h_2^3a_2 + \frac{1}{2}a_2h_2f_4 + \frac{7}{10}a_2^2a_{t,1} \right) r^4 + \mathcal{O}(r^5 \ln r), \quad (2.91)$$

$$\begin{aligned} V = & -h_2a_2 r^2 + \left( \frac{3}{2}a_{t,3} - \frac{5}{2}h_2^2a_{t,1} \right) r^3 + \left( -14h_2^3a_2 + \frac{1}{2}a_2h_2f_4 - \frac{13}{40}a_2^2a_{t,1} - \frac{3}{2}a_{t,1}f_{1,6} \right. \\ & \left. - \frac{3}{20}a_{t,1}a_2^2 \ln r \right) r^4 + \mathcal{O}(r^5 \ln r), \end{aligned} \quad (2.92)$$

$$\begin{aligned} H = & 1 + h_2 + \frac{1}{2}h_2^2 r^2 + \left( -\frac{3}{2}h_2^3 - \frac{1}{4}h_2f_4 - \frac{1}{4}a_2a_{t,1} \right) r^3 + \left( -\frac{13}{8}h_2^4 - \frac{1}{4}h_2^2f_4 \right. \\ & \left. - \frac{7}{60}a_2^2h_2 - \frac{1}{4}a_{t,1}h_2a_2 + \frac{1}{2}h_2f_{1,6} + \frac{1}{20}h_2a_2^2 \ln r \right) r^4 + \mathcal{O}(r^5 \ln r), \end{aligned} \quad (2.93)$$

specified by

$$\left\{ a_2, f_4, f_{1,6}, f_{1,8}, a_{t,1}, a_{t,3}, h_2 \right\}, \quad (2.94)$$

as functions of a  $U(1)_B$  chemical potential  $\mu$ ;

■ in the IR, *i.e.*, as  $y \equiv 1 - r \rightarrow 0_+$ ,

$$\begin{aligned} f_1 = & f_{1,0}^h + \mathcal{O}(y), & f_2 = & f_{2,0}^h + \mathcal{O}(y), & s = & s_0^h + \mathcal{O}(y), & H = & h_0^h + \mathcal{O}(y), \\ \Phi = & a_1^h y + \mathcal{O}(y^2), & A = & (a_{t,1}^h - 2a_{j,1}^h)y + \mathcal{O}(y^2), & V = & (a_{t,1}^h + a_{j,1}^h)y + \mathcal{O}(y^2), \\ f = & \left( \frac{2(s_0^h)^2}{(f_{2,0}^h)^8(f_{1,0}^h)^2} - \frac{(a_1^h - a_{j,1}^h)^2(h_0^h)^4}{2(f_{2,0}^h)^4(f_{1,0}^h)^2} - \frac{(a_1^h + a_{j,1}^h)^2}{2(f_{2,0}^h)^4(f_{1,0}^h)^2(h_0^h)^4} \right) y + \mathcal{O}(y^2), \end{aligned} \quad (2.95)$$

specified by

$$\left\{ s_0^h, f_{1,0}^h, f_{2,0}^h, a_1^h, a_{t,1}^h, a_{j,1}^h, h_0^h \right\}, \quad (2.96)$$

again, as functions of a  $U(1)_B$  chemical potential  $\mu$ . Note that in total, we have 7 parameters in the UV (2.94) and 7 parameters in the IR (2.96), precisely as needed to specify a solution of a coupled system of equations for the background fields:  $2 \times 6 + 1 \times 2 = 14$ .

Once the regular black brane solutions are constructed, we can use the holographic renormalization<sup>15</sup> to extract their thermodynamic properties:

$$\begin{aligned} 2\pi T &= \frac{2s_0^h}{(f_{2,0}^h)^8 (f_{1,0}^h)^2} - \frac{(a_1^h - a_{j,1}^h)^2 (h_0^h)^4}{2(f_{2,0}^h)^4 (f_{1,0}^h)^2 s_0^h} - \frac{(a_1^h + a_{j,1}^h)^2}{2(f_{2,0}^h)^4 (f_{1,0}^h)^2 (h_0^h)^4 s_0^h}, & \hat{\mathcal{E}} &\equiv 2\kappa_5^2 \mathcal{E} = -3f_4, \\ \hat{\rho}_B &\equiv 2\kappa_5^2 \rho_B = -4a_2, & \hat{\mathcal{S}} &\equiv 2\kappa_5^2 \mathcal{S} = 4\pi f_{1,0}^h (f_{2,0}^h)^4, & \hat{\Omega} &\equiv 2\kappa_5^2 \Omega = 4\mu a_2 - 3f_4 - T\hat{\mathcal{S}}, \\ \hat{\rho}_R &\equiv 2\kappa_5^2 \rho_R = -2a_{t,1}, & \hat{\mathcal{O}}_2 &\equiv 2\kappa_5^2 \mathcal{O}_2 = h_2, \end{aligned} \quad (2.97)$$

where  $T$  is the temperature,  $\mathcal{S}$  is the entropy density,  $\Omega$  is the Gibbs free energy density,  $\mathcal{E}$  is the energy density,  $\rho_B$  is the  $U(1)_B$  symmetry charge density,  $\rho_R$  is the  $U(1)_R$  symmetry charge density (it is nonzero even though the corresponding chemical potential  $\mu_R = 0$ ), and  $\mathcal{O}_2$  is the thermal expectation value of the dimension-2 operator dual to the bulk scalar  $H$ . The thermodynamics of R-charged baryonic black branes is explored in section 2.6.

An important check on the numerics is the verification of the thermodynamic constraints (2.45), presented in fig. 3. The left/right panel verifies constraint (A)/(B) of (2.45).

## 2.5 Non-perturbative instability of the baryonic black branes

It is known that the baryonic black branes reviewed in section 2.1 suffer from the nonperturbative D3- $\overline{\text{D3}}$  nucleation instability, provided [1]<sup>16</sup>

$$T \lesssim 0.2\sqrt{2} \mu. \quad (2.98)$$

---

<sup>15</sup>In this phase one should be careful with the holographic renormalization: even though there is no source term for the bulk mode  $H$ , the counterterms for the renormalization of the  $\Delta = 2$  mode are needed to insure the correct thermodynamics; see e.g., [23].

<sup>16</sup>See also [24, 25] for a related later work.

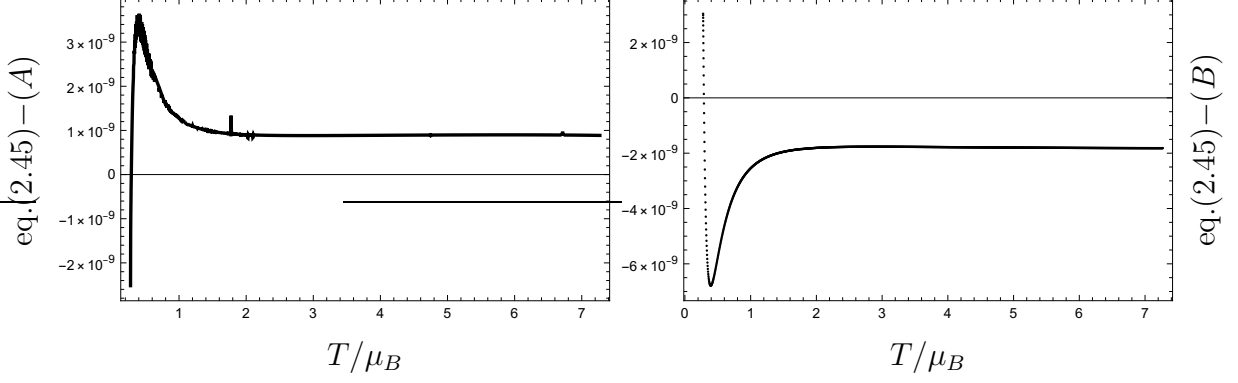


Figure 3: Numerical construction of  $R$ -charged baryonic black branes is in excellent agreement with the expected thermodynamic constraints of eq.(2.45).

The approximate sign in (2.98) does not allow to establish whether the critical temperature for the onset of this nucleation instability is above/below the critical temperature for the  $U(1)_R$  symmetry charge clumping instability (2.68). In this section we provide the precise evaluation of the critical temperature (2.98).

The effective action for the probe  $D3/\overline{D3}$  brane in generic type IIB supergravity background was studied in [26]. For a static<sup>17</sup> 3-brane of charge  $q$  (we use  $q = +1$  for a  $D3$  brane and  $q = -1$  for an  $\overline{D3}$  brane) with a world-volume along  $\partial\mathcal{M}_5$ :

$$S_{3-brane} = -T_3 \int_{\partial\mathcal{M}_5} d^4x \sqrt{\hat{g}} + qT_3 \int_{\partial\mathcal{M}_5} \hat{C}_4, \quad (2.99)$$

where  $T_3$  is the 3-brane tension;  $\hat{g}$  is the induced metric on the world-volume of the probe, see (2.7) with  $ds_5^2$  given by (2.29), (2.30),

$$\hat{g}_{\mu\nu} = \text{diag}(-c_1^2, c_2^2, c_2^2, c_2^2) = \text{diag}\left(-\frac{f}{r}, \frac{1}{r}, \frac{1}{r}, \frac{1}{r}\right), \quad (2.100)$$

and

$$d\hat{C}_4 = -\frac{2s}{f_1 f_2^4 r^3} \text{vol}_{R^{3,1}} \wedge dr. \quad (2.101)$$

From (2.99), the 3-brane effective potential  $\hat{V}_q \equiv \frac{V_q}{T_3}$  is thus

$$\hat{V}_q = \frac{\sqrt{f}}{r^2} + q \int^r d\rho \frac{2s}{f_1 f_2^4 \rho^3} + \text{const}, \quad (2.102)$$

<sup>17</sup>To compute a 3-brane potential it is sufficient to consider a 3-brane at a fixed radial location.

where the additive constant is such that the  $D3$  brane potential  $\hat{V}_+$  vanishes at the AdS boundary, *i.e.*, as  $r \rightarrow 0$ . It is easy to see that the  $\overline{D3}$  brane potential is always minimized at the baryonic black brane horizon; hence, a nucleated at some fixed radial location  $\overline{D3}$  brane will move towards the horizon. In what follows we study the  $D3$  brane effective potential  $\hat{V}_+$ .

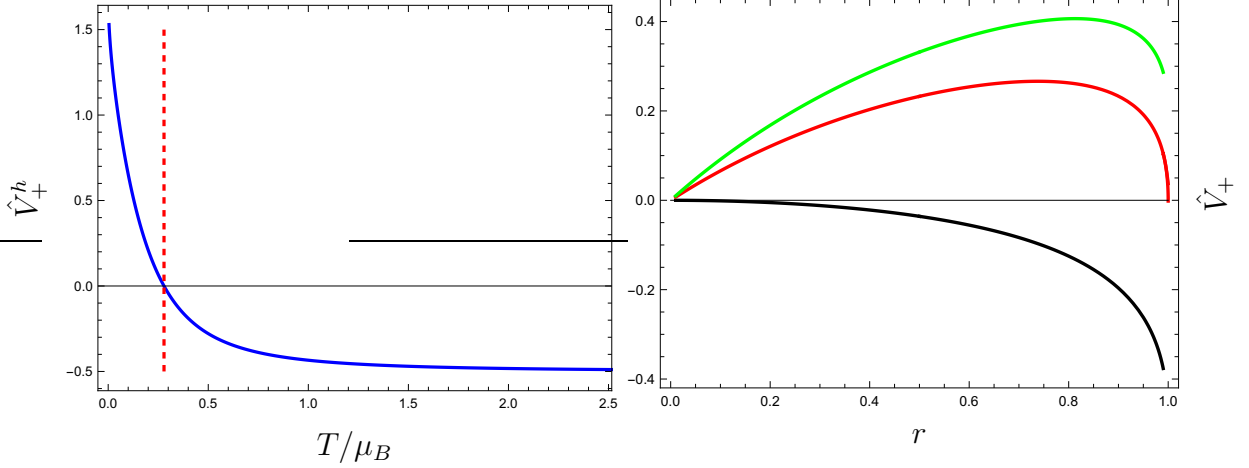


Figure 4: Potential of the probe  $D3$  brane at the baryonic black branes horizon as a function of  $T/\mu_B$  (the left panel). The vertical red dashed line is the critical temperature for the onset of the  $D3$ - $\overline{D3}$  nucleating instability, (2.106). The right panel: the typical  $D3$  brane potential  $\hat{V}_+(r)$  for  $\hat{V}_+^h < 0$  (the black curve), for  $\hat{V}_+^h = 0$  (the red curve), and for  $\hat{V}_+^h > 0$  (the green curve). The radial coordinate  $r$  ranges from the asymptotic AdS boundary  $r \rightarrow 0_+$ , to the baryonic black brane horizon  $r \rightarrow 1_-$ .

In practice, given a black brane background (2.29)-(2.43), we numerically solve the differential equation (from (2.102)),

$$0 = \frac{d\hat{V}_+}{dr} - \frac{f'}{2r^2\sqrt{f}} + \frac{2\sqrt{f}}{r^3} - \frac{2s}{f_1 f_2^4 r^3}, \quad (2.103)$$

subject to the following asymptotics:

- in the UV, *i.e.*, as  $r \rightarrow 0_+$ ,

$$\hat{V}_+ = a_2^2 r + \left( -\frac{1}{8}f_4^2 - 20f_{1,8} \right) r^2 + \mathcal{O}(r^3); \quad (2.104)$$

- in the IR, *i.e.*, as  $y \equiv 1 - r \rightarrow 0_+$ ,

$$\hat{V}_+ = \hat{V}_+^h + \frac{\sqrt{2(s_0^h)^2 - (a_1^h)^2(f_{2,0}^h)^4}}{f_{1,0}^h(f_{2,0}^h)^4} \sqrt{y} + \mathcal{O}(y), \quad (2.105)$$

where  $\hat{V}_+^h$  is the value of the probe  $D3$ -brane potential at the horizon of the baryonic black branes. The value of  $\hat{V}_+^h$  as a function of the baryonic chemical potential  $\mu$  is presented in fig. 4 (the left panel). A shape of a probe  $D3$  brane potential crucially depends on whether  $\hat{V}_+^h < 0$  or  $\hat{V}_+^h > 0$ , fig. 4 the right panel. In the former case, the global minimum of the potential is at the horizon, and it is near the horizon where the  $D3$ - $\overline{D3}$  probe brane pair will predominantly be nucleated, with both branes ‘falling through the horizon’ — in this case the baryonic black brane horizon is free from the ‘Fermi seasickness’ of [5]. On the contrary, when  $\hat{V}_+^h > 0$ , the global minimum of the  $D3$  brane potential is at the AdS boundary; as a result, for a  $D3$ - $\overline{D3}$  probe brane pair nucleation near the AdS boundary, the  $D3$  brane would escape to the asymptotic boundary, while the  $\overline{D3}$  will move towards the horizon, leading to the ‘Fermi seasickness’. The onset of this instability is precisely the value of the chemical potential, such that

$$\hat{V}_+^h \Big|_{T/\mu} = 0 \quad \iff \quad \frac{T}{\mu} = \frac{T}{\mu_B} \Big|_{non-pert} = 0.2789(9), \quad (2.106)$$

represented by the vertical red dashed line on the left panel of fig. 4.

## 2.6 Phases of the conifold gauge theory with $\mu_B \neq 0$ and $\mu_R = 0$

Strongly coupled conformal Klebanov-Witten gauge theory at finite baryonic chemical potential and vanishing  $R$ -symmetry chemical potential has two phases: a *disordered* phase (originally constructed in [1] and reviewed in section 2.1), and the *ordered* phase constructed in section 2.4. The ordered phase is called so, as it has a non-vanishing thermal expectation value of the dimension-2 operator; furthermore, it has a nonzero  $R$ -symmetry charge.

The phase diagram of the conifold gauge theory at finite baryonic chemical potential  $\mu_B$  is presented in fig. 5. The red dot indicates the critical temperature (1.1). The disordered phase (the solid blue lines) exists for arbitrary temperatures; in the extremal limit  $\frac{T}{\mu_B} \rightarrow 0$  it has finite energy and entropy densities (the right panel, green dot). The ordered phase (the solid black lines) is exotic [27–29] — it originates at the criticality,

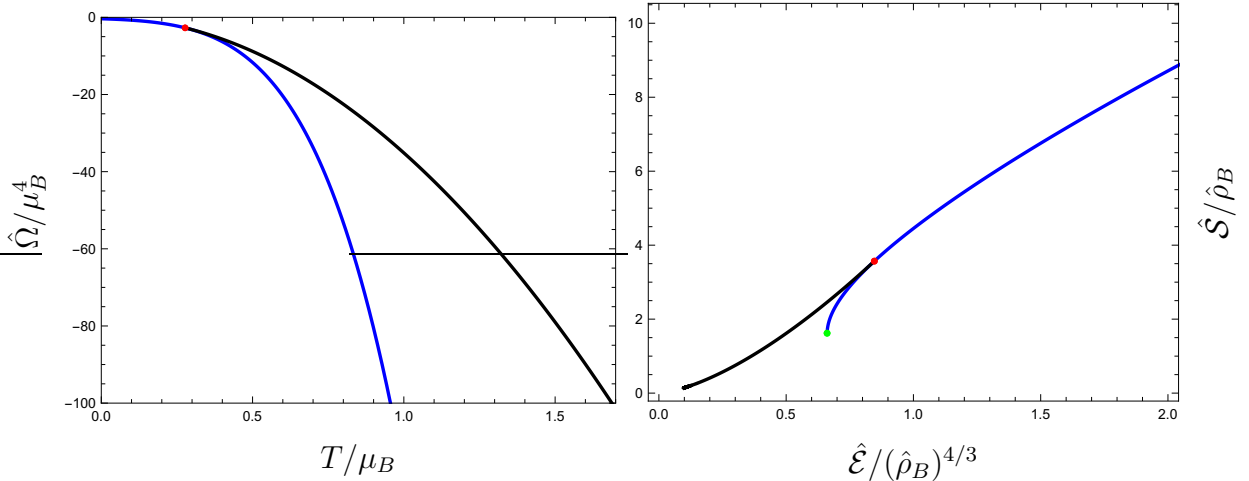


Figure 5: The Gibbs free energy densities  $\hat{\Omega}$  (the right panel) and the entropy densities  $\hat{S}$  of the disordered (the solid blues curves) and the ordered (the solid black curves) phases as functions of temperature  $T$  and the energy densities  $\hat{\mathcal{E}}$  correspondingly. The baryonic chemical potential  $\mu_B$  (or the baryonic charge density  $\hat{\rho}_B$ ) is kept fixed. The red dot represents the critical temperature/energy density (1.1). The green dot (the right panel) represents the extremal limit of the baryonic black branes.

however it extends to higher, rather than the lower temperatures. The ordered phase is subdominant in the grand canonical ensemble (the left panel); however, it has higher entropy density at the same value of the baryonic charge density than the disordered phase (the right panel). The right panel is not a genuine microcanonical ensemble since the disordered phase always has zero charge density of the  $U(1)_R$  symmetry, while the ordered phase carries a nontrivial charge density  $\hat{\rho}_R \neq 0$ .

Fig. 6 explores the critical regime: the left panel shows the difference between the Gibbs free energy densities of the ordered and the disordered phases, and the right panel shows the thermal expectation value of the dimension-2 operator  $\hat{\mathcal{O}}_2$  in the near-critical regime of the ordered phase. The red dashed lines have slopes 2 and  $\frac{1}{2}$  in the left/right panels correspondingly. Thus, close to criticality, *i.e.*, for  $(T - T_{crit}) \ll T_{crit}$ ,

$$(\hat{\Omega}_{ord} - \hat{\Omega}_{dis}) \propto \mu_B^2 (T - T_{crit})^2, \quad \hat{\mathcal{O}}_2 \propto \mu_B^{3/2} \sqrt{T - T_{crit}}. \quad (2.107)$$

The ordered phase appears to extend to arbitrary high temperatures - it is another example of the conformal ordered phase in the presence of chemical potential [10, 11]<sup>18</sup>.

<sup>18</sup>Charge neutral conformal order was recently studied in [13, 30–36].

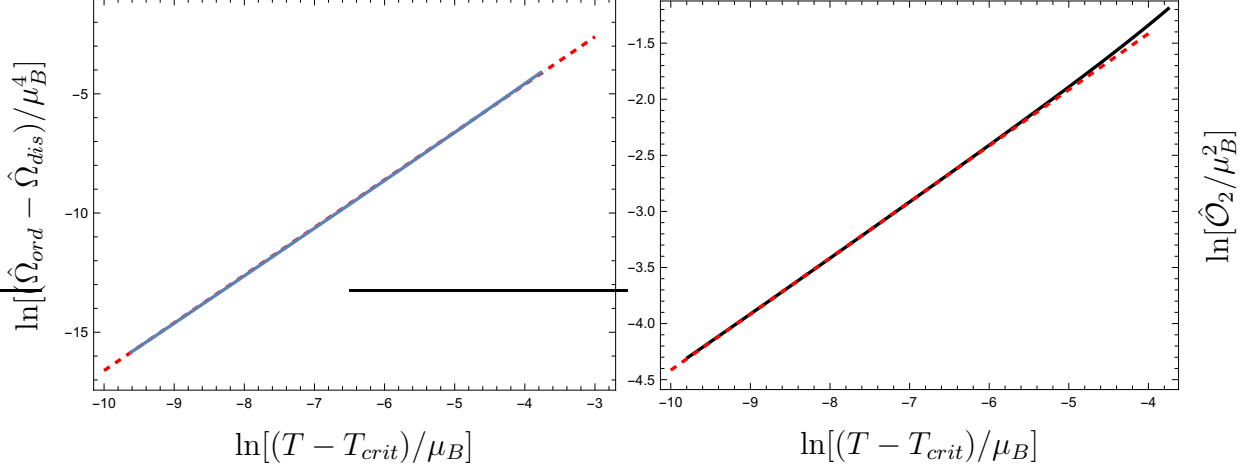


Figure 6: The near-critical behavior,  $(T - T_{crit}) \ll T_{crit}$  of the disordered and ordered phases (the left panel). The right panel shows the critical behavior of the order parameter: the expectation value of the dimension-2 operator  $\hat{\mathcal{O}}_2$ . The red dashed lines have slopes implying the scaling relation as in (2.107).

In fig. 7 we show the large  $\frac{T}{\mu_B}$  scaling of the energy density  $\hat{\mathcal{E}}$  (the left panel) and the order parameter  $\hat{\mathcal{O}}_2$  (the right panel) of the ordered phase. The slope of the red dashed line is 2, implying that

$$\hat{\mathcal{E}} \propto \mu_B^2 T^2, \quad \text{as } T \gg \mu_B, \quad (2.108)$$

while

$$\hat{\mathcal{O}}_2 \propto T^2, \quad \text{as } T \gg \mu_B. \quad (2.109)$$

This is identical scaling to that of the ordered phase of the  $\mathcal{N} = 4$  SYM plasma [10,11]. We verified that the scaling of the remaining thermodynamic quantities is consistent with the first law of thermodynamics, give (2.108):

$$\hat{\Omega} \propto -\mu_B^2 T^2, \quad \hat{\mathcal{S}} \propto \mu_B^2 T, \quad \rho_B \propto \mu_B T^2. \quad (2.110)$$

The ordered phase has a finite charge density  $\hat{\rho}_R$  under the  $U(1)_R$  global symmetry. This charge density can be viewed as another order parameter distinguishing the disordered and the ordered phases of the conifold gauge theory. In the left panel of fig. 8 we show the near-critical scaling of the  $R$ -symmetry charge density, while in the right panel we show that  $\rho_R \propto \rho_B$  as  $T \gg \mu_B$ . The slope/offset of the red dashed lines in

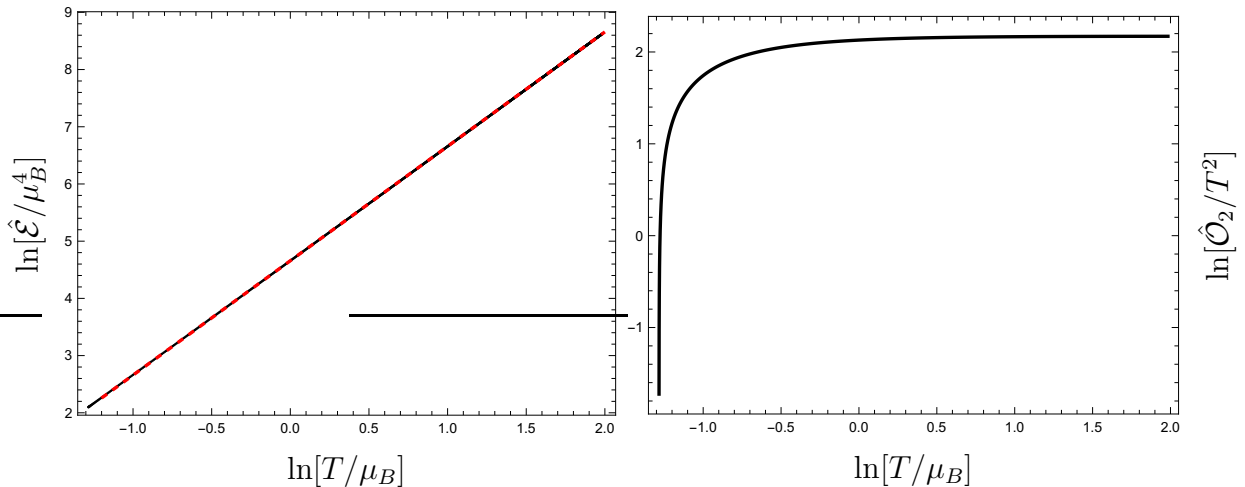


Figure 7: The scaling of the ordered phase energy density  $\hat{\mathcal{E}}$  (the left panel) and the order parameter  $\hat{\mathcal{O}}_2$  (the right panel) as  $T \gg \mu_B$ . The slope of the red dashed line implies the energy density scaling (2.108).

the left/right panels imply

$$\frac{\rho_R}{\rho_B} = \begin{cases} \propto \left(\frac{T-T_{crit}}{\mu_B}\right)^{1/2}, & \text{as } (T - T_{crit}) \ll T_{crit}, \\ \frac{1}{3}, & \text{as } T \gg \mu_B. \end{cases} \quad (2.111)$$

## Acknowledgments

I would like to thank Igor Klebanov for communications, and the referee for encouraging revising the "Fermi seasickness" instability of the baryonic black branes. Research at Perimeter Institute is supported by the Government of Canada through Industry Canada and by the Province of Ontario through the Ministry of Research & Innovation. This work was further supported by NSERC through the Discovery Grants program.

## References

- [1] C. P. Herzog, I. R. Klebanov, S. S. Pufu and T. Tesileanu, *Emergent Quantum Near-Criticality from Baryonic Black Branes*, *JHEP* **03** (2010) 093, [0911.0400].
- [2] I. R. Klebanov and E. Witten, *Superconformal field theory on three-branes at a Calabi-Yau singularity*, *Nucl. Phys.* **B536** (1998) 199–218, [hep-th/9807080].

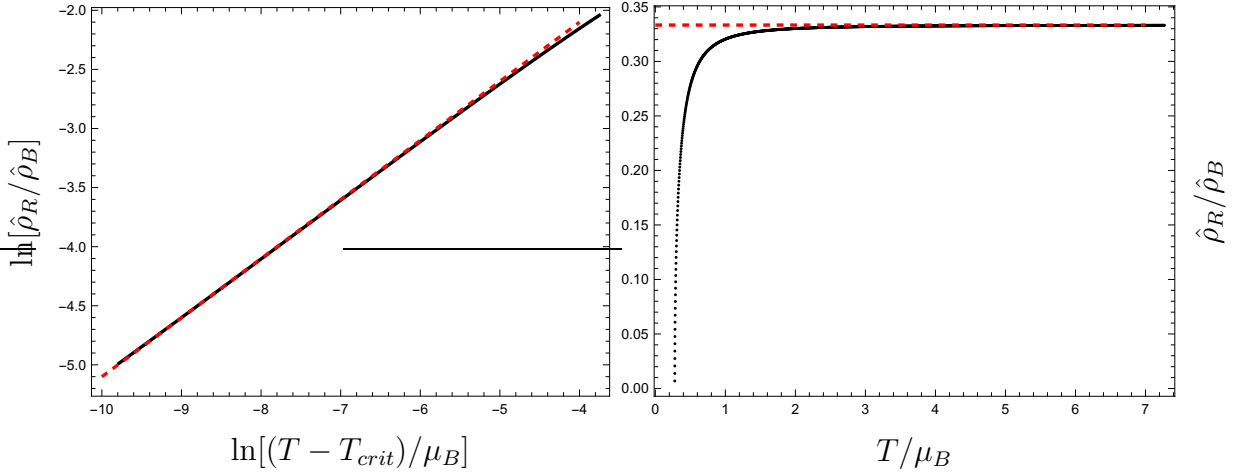


Figure 8:  $R$ -symmetry charge density  $\hat{\rho}_R$  in the ordered phase is yet another order parameter distinguishing this phase from the disordered one (the left panel). The slope of the red dashed line implies the scaling relation (2.111). As  $T \gg \mu_B$  the baryonic and the  $R$ -symmetry charge densities become proportional to each other (the right panel). The horizontal dashed red line is at  $\frac{1}{3}$ .

- [3] A. Buchel, *Fluxification and scalarization of the conifold black holes*, 2411.15950.
- [4] S. S. Gubser, C. P. Herzog, S. S. Pufu and T. Tesileanu, *Superconductors from Superstrings*, *Phys. Rev. Lett.* **103** (2009) 141601, [0907.3510].
- [5] S. A. Hartnoll, J. Polchinski, E. Silverstein and D. Tong, *Towards strange metallic holography*, *JHEP* **04** (2010) 120, [0912.1061].
- [6] L. Gladden, V. Ivo, P. Kovtun and A. O. Starinets, *Instability in  $\mathcal{N} = 4$  supersymmetric Yang-Mills theory at finite density*, 2412.12353.
- [7] A. Ceresole, G. Dall’Agata, R. D’Auria and S. Ferrara, *Spectrum of type IIB supergravity on  $AdS(5) \times T^{**}11$ : Predictions on  $N=1$  SCFT’s*, *Phys. Rev. D* **61** (2000) 066001, [hep-th/9905226].
- [8] D. Cassani and A. F. Faedo, *A Supersymmetric consistent truncation for conifold solutions*, *Nucl. Phys. B* **843** (2011) 455–484, [1008.0883].
- [9] A. Buchel, *Effective Action of the Baryonic Branch in String Theory Flux Throats*, *JHEP* **09** (2014) 117, [1405.1518].

- [10] A. Buchel, *The ordered phase of charged  $N=4$  SYM plasma*, 2501.01856.
- [11] A. Buchel, *The ordered phase of charged  $N=4$  SYM plasma from STU*, 2501.12403.
- [12] A. Buchel, *A Holographic perspective on Gubser-Mitra conjecture*, *Nucl. Phys.* **B731** (2005) 109–124, [hep-th/0507275].
- [13] A. Buchel, *Fate of the conformal order*, *Phys. Rev. D* **103** (2021) 026008, [2011.11509].
- [14] R. Minasian and D. Tsimpis, *On the geometry of nontrivially embedded branes*, *Nucl. Phys. B* **572** (2000) 499–513, [hep-th/9911042].
- [15] A. Buchel and J. T. Liu, *Gauged supergravity from type IIB string theory on  $Y^{**p,q}$  manifolds*, *Nucl. Phys. B* **771** (2007) 93–112, [hep-th/0608002].
- [16] O. Aharony, A. Buchel and P. Kerner, *The Black hole in the throat: Thermodynamics of strongly coupled cascading gauge theories*, *Phys. Rev.* **D76** (2007) 086005, [0706.1768].
- [17] V. Balasubramanian and P. Kraus, *A Stress tensor for Anti-de Sitter gravity*, *Commun. Math. Phys.* **208** (1999) 413–428, [hep-th/9902121].
- [18] P. K. Kovtun and A. O. Starinets, *Quasinormal modes and holography*, *Phys. Rev. D* **72** (2005) 086009, [hep-th/0506184].
- [19] D. T. Son and A. O. Starinets, *Minkowski space correlators in AdS / CFT correspondence: Recipe and applications*, *JHEP* **09** (2002) 042, [hep-th/0205051].
- [20] O. Henriksson, C. Hoyos and N. Jokela, *Novel color superconducting phases of  $\mathcal{N} = 4$  super Yang-Mills at strong coupling*, *JHEP* **09** (2019) 088, [1907.01562].
- [21] A. Anabalón and J. Oliva, *Plasma-Plasma Third Order Phase Transition from Type IIB Supergravity*, *Phys. Rev. Lett.* **133** (2024) 121601, [2405.04611].
- [22] A. Buchel,  $\chi$ SB of cascading gauge theory in de Sitter, *JHEP* **05** (2020) 035, [1912.03566].

- [23] A. Buchel, L. Lehner and R. C. Myers, *Thermal quenches in  $N=2^*$  plasmas*, *JHEP* **08** (2012) 049, [1206.6785].
- [24] O. Henriksson, C. Hoyos and N. Jokela, *Brane nucleation instabilities in non-AdS/non-CFT*, *JHEP* **02** (2020) 007, [1910.06348].
- [25] O. Henriksson, N. Jokela and J. Junttila, *Dynamics of a Higgs phase transition in the Klebanov-Witten theory*, *JHEP* **04** (2025) 051, [2411.19667].
- [26] A. Buchel, *Gauge theories on hyperbolic spaces and dual wormhole instabilities*, *Phys. Rev. D* **70** (2004) 066004, [hep-th/0402174].
- [27] A. Buchel and C. Pagnutti, *Exotic Hairy Black Holes*, *Nucl. Phys. B* **824** (2010) 85–94, [0904.1716].
- [28] A. Buchel, *Singularity development and supersymmetry in holography*, *JHEP* **08** (2017) 134, [1705.08560].
- [29] A. Buchel, *Klebanov-Strassler black hole*, *JHEP* **01** (2019) 207, [1809.08484].
- [30] N. Chai, S. Chaudhuri, C. Choi, Z. Komargodski, E. Rabinovici and M. Smolkin, *Thermal Order in Conformal Theories*, *Phys. Rev. D* **102** (2020) 065014, [2005.03676].
- [31] A. Buchel, *SUGRA/Strings like to be bald*, *Phys. Lett. B* **814** (2021) 136111, [2007.09420].
- [32] A. Buchel, *Thermal order in holographic CFTs and no-hair theorem violation in black branes*, *Nucl. Phys. B* **967** (2021) 115425, [2005.07833].
- [33] N. Chai, A. Dymarsky, M. Goykhman, R. Sinha and M. Smolkin, *A model of persistent breaking of continuous symmetry*, *SciPost Phys.* **12** (2022) 181, [2111.02474].
- [34] S. Chaudhuri and E. Rabinovici, *Symmetry breaking at high temperatures in large  $N$  gauge theories*, *JHEP* **08** (2021) 148, [2106.11323].
- [35] A. Buchel, *The quest for a conifold conformal order*, *JHEP* **08** (2022) 080, [2205.00612].

- [36] N. Chai, A. Dymarsky and M. Smolkin, *Model of Persistent Breaking of Discrete Symmetry*, *Phys. Rev. Lett.* **128** (2022) 011601, [2106.09723].